Semiclassical theory of bipolaronic superconductivity in a bond-modulated electron-phonon model

Kyung-Su Kim,[1,*,†] Zhaoyu Han [1,*,‡] and John Sous [1,2,§]

[1]*Department of Physics, Stanford University, Stanford, California 93405, USA*
[2]*Department of Chemistry and Biochemistry, University of California, San Diego, La Jolla, California 92093, USA*

We analyze the transition temperature T_c of bipolaronic superconductivity in a bond Su-Schrieffer-Heeger (bond-SSH) model—also known as a bond Peierls model—where bond phonons modulate the electron hoppings. Using a semiclassical instanton approximation justifiable in the adiabatic limit of slow phonons, we find that the bipolaron mass is only weakly enhanced in contrast to the typically large mass enhancement found in models where the phonons couple to electron density. Strikingly, in the "atomic" limit, we find a bond bipolaron can freely slide within a continuously degenerate energy manifold, explaining the origin of the weak mass enhancement in the strong coupling limit. A gas of these bipolarons can undergo a superfluid transition at a critical temperature for which we obtain an upper bound. This bound is exponentially larger than that in the Holstein model. Our study provides an analytical understanding of the mechanism behind the high-T_c bipolaronic superconductivity numerically observed in [Phys. Rev. X **13**, 011010 (2023)].

Introduction. The quest for higher critical transition-temperature (T_c) superconductivity has been of extensive interest, because of both fundamental theoretical importance and practical real-world applications [1]. It is known that the conventional Bardeen-Cooper-Schrieffer (BCS) mechanism of superconductivity leads to a relatively low value of T_c due to an exponential suppression in the regime of weak electron-phonon coupling strength (characterized by an energy scale $U_{e\text{-ph}}$). On the other hand, the value of T_c is also believed to be suppressed in the strong-coupling regime (large $U_{e\text{-ph}}$) due to the formation of bipolarons with large mass [2–7]. This suppression of T_c in both the weak and strong coupling limits was used to obtain an empirical bound on its value: $k_B T_c \lesssim 0.1 \cdot \hbar\omega$ [2,8–11] (where ω is the characteristic phonon frequency), the maximum of which is believed to arise at the "sweet spot" of intermediate $U_{e\text{-ph}}$.

The supposed "suppression" of T_c in the strong-coupling regime is based on the reasoning that the bipolarons always suffer from severe mass enhancement, which renders their dynamics rather slow. Such an expectation was challenged in recent numerical studies of the bond Peierls/Su-Schrieffer-Heeger (bond-SSH) model [12,13], which reported unusually weak enhancement of the bipolaron mass [14] and a concomitant large value of T_c that exceeds the aforementioned empirical bound. In this Letter, we aim to give an explanation for this unusual enhancement of T_c with a controllable analysis in the adiabatic limit of slow phonons, which is of relevance to real materials. Our main findings are as follows. (i) We show that the bipolaron mass remains unusually small.

(ii) We unveil a semiclassical picture behind the very weak mass enhancement: precisely, we find that in the limit of zero bare hopping t, there exists a degenerate manifold of bipolaron states within which a bipolaron can slide freely without any energy cost. The inclusion of a small bare hopping lifts the degeneracy and leads to a finite but small energy barrier, resulting in a weak mass enhancement. Thus, surprisingly, the suppression of T_c is least severe in the "atomic limit" ($t = 0$) corresponding to a trivial flat band. (iii) We estimate the bipolaron mass and radius to obtain an empirical bound on the value of T_c of the bipolaronic superconductivity, showing that it can be much larger than that in the standard cases where the phonons couple to electron density. (We explicitly make this comparison to the Holstein model). Our results provide an analytic understanding of recent numerical results on the bipolaronic high-T_c superconductivity found in the bond-SSH model in the dilute limit [12,13] and may shed light on superconductivity near half filling [15–17]. In a broader view, we hope our work provides another concrete example of various unexpected phenomena driven by strong bond-modulated electron-phonon coupling [17–31].

Model and methods. We study the bond-SSH model on a two-dimensional square lattice described by the Hamiltonian:

$$\hat{H} = \hat{H}_e + \hat{H}_{\text{ph}}, \tag{1}$$

$$\hat{H}_e = -\sum_{\langle ij \rangle, \sigma} (t + \alpha \hat{X}_{\langle ij \rangle})(\hat{c}_{i\sigma}^\dagger \hat{c}_{j\sigma} + \text{H.c.}), \tag{2}$$

$$\hat{H}_{\text{ph}} = \sum_{\langle ij \rangle} \left(\frac{K \hat{X}_{\langle ij \rangle}^2}{2} + \frac{\hat{P}_{\langle ij \rangle}^2}{2M} \right), \tag{3}$$

where the coordinates of the phonons $\hat{X}_{\langle ij \rangle}$ live on nearest-neighbor bonds $\langle ij \rangle$. Each local phonon mode has a frequency $\omega_0 \equiv \sqrt{K/M}$. Besides t and $\hbar\omega_0$, there is only one independent energy scale in this problem, $U_{e\text{-ph}} \equiv \alpha^2/K$, which

*These authors contributed equally to this work.
†Contact author: kyungsu@stanford.edu
‡Contact author: zyhan@stanford.edu
§Contact author: jsous@ucsd.edu

characterizes the strength of the electron-phonon coupling [32]. We set the lattice constant $a = 1$. Without loss of generality, we will consider the $t > 0$ case throughout the paper.

We analyze the problem in the adiabatic limit $\hbar\omega_0/U_{e\text{-ph}} \to 0$ for dilute electron concentrations, where two electrons form a bound bipolaron and move around with the help of phonons. As we will show, this situation is effectively described by a gas of repulsively interacting bosons, which undergo a superfluid transition at a temperature T_c [33–35]. We will first solve the problem in the static (classical) limit where $\omega_0 = 0$ ($M = \infty$). In such a case, one can obtain the electronic ground state energy in the two-electron sector,

$$\hat{V}_{\text{eff}}(\{\hat{X}_{\langle ij \rangle}\}) = 2\epsilon_0(\{\hat{X}_{\langle ij \rangle}\}) + \sum_{\langle ij \rangle} \frac{K\hat{X}_{\langle ij \rangle}^2}{2}, \quad (4)$$

where $2\epsilon_0(\{\hat{X}_{\langle ij \rangle}\})$ is the ground state energy of $\hat{H}_e$ in the two-electron sector for a given phonon configuration $\{\hat{X}_{\langle ij \rangle}\}$. We then minimize $\hat{V}_{\text{eff}}$ with respect to $\{X_{\langle ij \rangle}\}$ to obtain the bipolaron bound state with the smallest energy. Such bipolaron states, localized around different sites, are classically degenerate. For a small but finite phonon frequency $\omega_0 > 0$, these bipolarons acquire quantum dynamics described by the effective Hamiltonian

$$\hat{H}_{\text{eff}} = \hat{V}_{\text{eff}} + \sum_{\langle ij \rangle} \frac{\hat{P}_{\langle ij \rangle}^2}{2M}. \quad (5)$$

We will use a semiclassical instanton approximation to calculate the effective hopping of the bipolaron, which in turn gives an expression for the bipolaron effective mass m^*. From this, we estimate the value of the critical temperature T_c of superconductivity of a gas of these bosonic bipolarons, which is given by [33–35]

$$T_c \approx C \frac{\hbar^2 \rho}{m^* k_B}, \quad (6)$$

where $C \equiv \frac{2\pi}{\ln(\frac{380}{4\pi})} \approx 1.84$. The maximum possible T_c is achieved for the density of electrons at which bipolarons start to overlap, $\rho = \frac{1}{\pi R^2}$, where R is the linear size of the bipolaron. We note that this T_c is not determined by the pairing energy scale as in the case of BCS or Migdal-Eliashberg theory [11], but rather by the phase coherence energy scale within the Bose-Einstein condensation (BEC) picture of preformed pairs.

Static limit. In the static (classical) limit where the phonon kinetic energy is neglected ($\omega_0 = 0$), we perform numerical optimization [36] to find the phonon configurations that minimize the effective potential $V_{\text{eff}}(\{X_{\langle ij \rangle}\})$. We first consider the case corresponding to two electrons in the system. For the special case when $t = 0$, we obtain a manifold of degenerate bipolaron configurations localized around each site i. Such a manifold is parametrized by four phonon coordinates $X_{\langle ii_k \rangle}$ ($k = 1, 2, 3, 4$), where $i_1, ..., i_4$ are four nearest-neighbor sites connected to the site i (other phonon coordinates are zero). Minimizing the electronic energy within such phonon config-
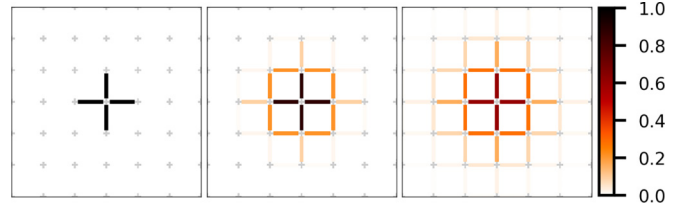

FIG. 1. The phonon configuration $\{X_{\langle ij \rangle}\}$ (measured in units of α/K) around a static bipolaron ($\omega_0 = 0$) for different values of $t/U_{e\text{-ph}} = 0.01$ (left), 0.35 (middle), and 0.7 (right).

urations, one obtains

$$V_{\text{eff}}(\{X_{\langle ij \rangle}\}) = -2\alpha \left[\sum_{k=1}^{4} X_{\langle ii_k \rangle}^2\right]^{\frac{1}{2}} + \frac{K}{2} \sum_{k=1}^{4} X_{\langle ii_k \rangle}^2, \quad (7)$$

with the electronic eigenfunction $|\Psi_{i,\sigma=\uparrow,\downarrow}^0(\{X\})\rangle$ with support on five sites i, i_1, i_2, i_3, and i_4. $V_{\text{eff}}(\{X_{\langle ij \rangle}\})$ is minimized when

$$\left[\sum_{k=1}^{4} X_{\langle ii_k \rangle}^2\right]^{\frac{1}{2}} = \frac{2\alpha}{K} \quad (8)$$

with energy $-2U_{e\text{-ph}}$. This degenerate manifold of bipolaron configurations means that the bipolaron can "slide" freely from one site to the other by deforming its configuration within the manifold. This exact behavior, found in the $t = 0$ limit, explains the origin of the small bipolaron mass, which extends to the regime of small but nonzero t (as we will see below), and, therefore, is (approximately) responsible for the numerically found behavior of a small mass in the strong-coupling limit $t/U_{e\text{-ph}} \lesssim 1$ [12–14].

Including a $t > 0$ term determines the unique lowest energy bipolaron configuration. In the small-t limit, first-order perturbation theory gives an energy correction for each configuration $\{X_{\langle ii_k \rangle}\}$ within the manifold, splitting the energies of different bipolaron configurations (8):

$$\Delta E = -2t\langle\Psi_{i,\uparrow}^e| \sum_{\langle ij \rangle} c_{i,\uparrow}^\dagger c_{j,\uparrow} |\Psi_{i,\uparrow}^e\rangle + O(t^2)$$

$$= -\frac{t}{\alpha/K} \sum_{k=1}^{4} X_{\langle ii_k \rangle} \geqslant -4t. \quad (9)$$

Here, the energy minimum (equality) is attained for the uniform "cross" configuration $X_{\langle ii_k \rangle} = \alpha/K$ (see the left panel of Fig. 1). Note that bipolarons centered around different sites are related by a lattice translation and are thus classically degenerate.

With increasing $t/U_{e\text{-ph}}$, bipolarons become more and more extended (see Fig. 1). To better quantify this observation, we compute the inverse participation ratio (IPR $\equiv \sum_i |\Psi_{i,\sigma}^0|^4$ [37]) of the electronic ground state $|\Psi_{i,\sigma}^0\rangle$ of $\hat{H}_e$ within the optimal $\{X_{\langle ij \rangle}\}$ and use this quantity to define an effective radius of the bipolaron

$$R \equiv \frac{1}{\sqrt{\pi(\text{IPR})}}. \quad (10)$$

Interestingly, we find that the size of the bipolaron remains rather small even for the largest $t/U_{e\text{-ph}} = 0.7$ considered.
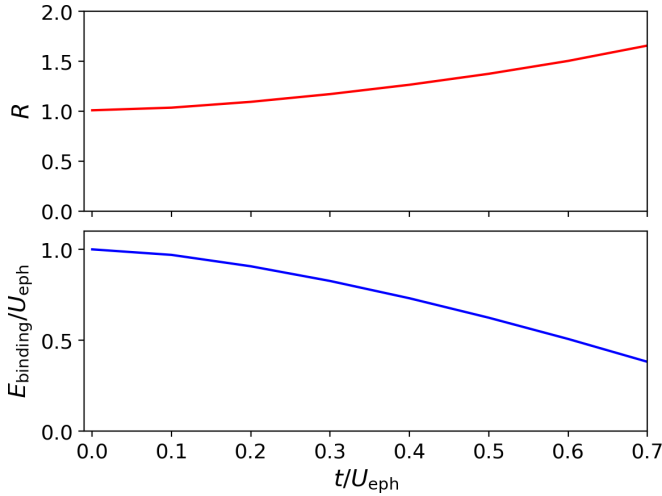
FIG. 2. The properties of bipolarons in the static limit $\omega_0 = 0$. We plot the effective radius R of the bipolaron [Eq. (10)] in the upper panel and the binding energy E_{binding} [Eq. (11)] in units of $U_{e\text{-ph}}$ in the lower panel as functions of the dimensionless constant $t/U_{e\text{-ph}}$.

Another meaningful quantity is the energy gain associated with the formation of a bipolaron, defined as

$$E_{\text{binding}} = 2E_{\text{polaron}} - E_{\text{bipolaron}}, \tag{11}$$

where E_{polaron} is the ground state energy in the single-electron sector. We plot these two quantities as a function of $t/U_{e\text{-ph}}$ in Fig. 2 [38].

Importantly, when considering a finite, but dilute density of electrons in the system, we find that they always tend to repel each other and phase separation does not preempt the superconducting phase [39].

Adiabatic limit. When a finite but small phonon kinetic energy is considered (i.e., $\hbar\omega_0/U_{e\text{-ph}} \to 0$), the classically degenerate bipolaron configurations centered at different sites become connected by quantum tunneling. The bipolaron hopping matrix element can be computed using the standard semiclassical instanton approximation in the two-electron sector,

$$\tau_{\text{eff}} = \hbar\omega_0 \, A \sqrt{\frac{S_{\text{inst}}}{2\pi}} e^{-S_{\text{inst}}}, \tag{12}$$

where S_{inst} is the action of the semiclassical path that connects the initial (init) and the final (final) bipolaron configurations,

$$S_{\text{inst}} \equiv \frac{U_{e\text{-ph}}}{\hbar\omega_0} \tilde{S} = \min \int_{X_{\text{init}}}^{X_{\text{final}}} dX \sqrt{2M[V_{\text{eff}}(X) - E_0]}, \tag{13}$$
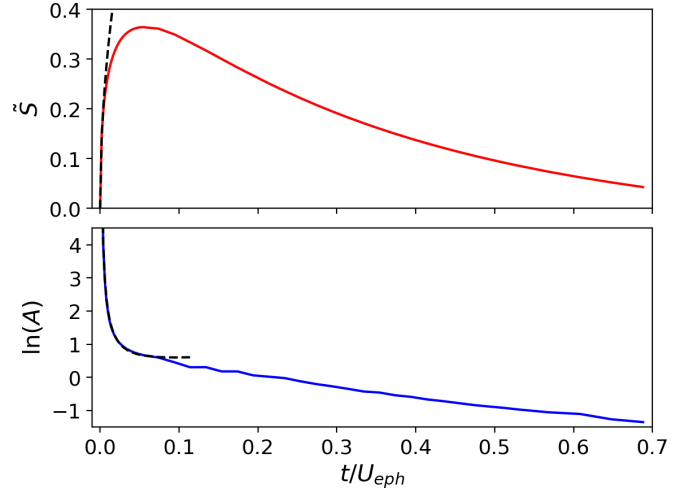

FIG. 4. The energetics of bipolaron hopping. We plot the normalized classical action of the nearest-neighbor tunneling process, $\tilde{S} \equiv \frac{\hbar\omega_0}{U_{e\text{-ph}}} S_{\text{inst}}$, in the upper panel, and the leading-order fluctuational correction to it, $\ln(A)$, in the lower panel. In the small $t/U_{e\text{-ph}}$ limit, we find that the numerical results are well fitted by $\tilde{S} \approx 3.2\sqrt{t/U_{e\text{-ph}}}$ (upper panel) and $\ln(A) \approx \ln(2.4) + \frac{3}{4}\ln\frac{t}{U_{e\text{-ph}}} + 0.46\sqrt{\frac{U_{e\text{-ph}}}{t}}$ (lower panel) which are drawn as dashed lines.

where $E_0 \equiv V_{\text{eff}}(X_{\text{init}}) = V_{\text{eff}}(X_{\text{final}})$ is the classical energy of a bipolaron (see Fig. 3 for an exemplary trajectory). A is the "fluctuation determinant," the subleading fluctuational correction, that captures Gaussian fluctuation around the semiclassical tunneling path

$$A = \left[\frac{\omega_0^2 \, \widetilde{\det}\big(-\partial_\tau^2 + \frac{1}{M}V_{\text{eff}}''[X_{\text{cl}}(\tau)]\big)}{\det\big(-\partial_\tau^2 + \frac{1}{M}V_{\text{eff}}''[X_{\text{init}}]\big)}\right]^{-\frac{1}{2}}. \tag{14}$$

Here, $\widetilde{\det}$ is the determinant without the zero eigenvalue [40–42], $X_{\text{cl}}(\tau)$ is the instanton trajectory and the double prime denotes the second functional derivative of $V_{\text{eff}}[X(\tau)]$. We only consider a nearest-neighbor hopping matrix element, since further-ranged tunneling processes will be exponentially smaller in the $\omega_0 \to 0$ limit. We numerically evaluate the normalized instanton action $\tilde{S}$ and A as a function of $t/U_{e\text{-ph}}$ in Fig. 4 (see Refs. [43,44] for details of their calculation). The effective bipolaron mass can in turn be estimated as $m^* = \frac{\hbar^2}{4\tau_{\text{eff}}}$, which can be substituted into Eq. (6) to yield an estimate for the value of T_c. Note that further including the effects of longer-ranged hoppings of bipolarons will make m^* smaller and therefore T_c higher.
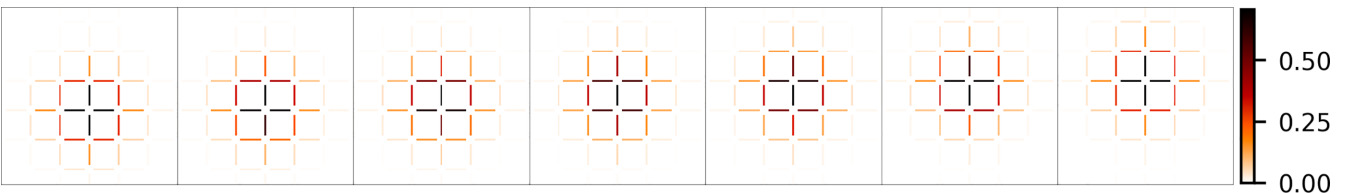

FIG. 3. Snapshots of an imaginary time tunneling trajectory at seven representative time slices connecting the initial (leftmost panel) and the final (rightmost panel) bipolaron configurations. The color encodes the configuration of the phonon displacement $\{X_{(ij)}\}$ (measured in unit of α/K). This simulation is performed for $t/U_{e\text{-ph}} = 0.6$.

Empirical bound on T_c. The maximum possible value of T_c from Eq. (6) arises for the density at which bipolarons start to overlap $\rho_{\max} \sim \frac{1}{\pi R^2}$:

$$k_B T_c^{\max} \sim \frac{\sqrt{\hbar\omega_0 U_{e\text{-ph}}}}{R^2} A \sqrt{\frac{\tilde{S}}{2\pi}} \, e^{-\frac{U_{e\text{-ph}}}{\hbar\omega_0}\tilde{S}}. \quad (15)$$

We find that $\tilde{S} < 0.35$ which is much smaller than the corresponding quantity in the Holstein model with density coupling $\alpha \sum_i X_i n_i$, $\tilde{S}^{\text{Holstein}} = 2$ [45]. This implies that the value of T_c in the bond model can be exponentially larger than that in the Holstein model in the adiabatic limit $\hbar\omega_0/U_{e\text{-ph}} \to 0$.

In the limit $t/U_{e\text{-ph}} \to 0$, we further obtain the asymptotic behaviors of the action and the fluctuation determinant: $\tilde{S} \approx 3.2\sqrt{\frac{t}{U_{e\text{-ph}}}} \to 0$ and $A \approx 2.4 \cdot (\frac{t}{U_{e\text{-ph}}})^{3/4} e^{0.46 \cdot \sqrt{\frac{U_{e\text{-ph}}}{t}}} \to \infty$, as shown in Fig. 4. That is, as $t/U_{e\text{-ph}} \to 0$, the tunnel barrier between the two neighboring bipolaron configurations tends to zero and the fluctuation determinant diverges. This is due to the continuous family of degenerate bipolaron configurations [Eq. (8)]. For $t = 0$, the two nearest-neighbor "cross" bipolaron configurations are connected by a zero tunnel barrier through Eq. (8). For small t, the first order correction in the energy of noncross configuration is $\Delta E = O(t)$, and hence the tunnel barrier height $\Delta V_{\text{eff}} \sim t$. On the other hand, the tunnel distance in coordinate space $\Delta X \sim \alpha/K$. Therefore,

$$\tilde{S} \sim \frac{\hbar\omega_0}{U_{e\text{-ph}}} \Delta X \sqrt{2M \Delta V_{\text{eff}}} \sim \sqrt{\frac{t}{U_{e\text{-ph}}}}. \quad (16)$$

Moreover, the instanton duration $\Delta \tau_{\text{inst}}$ in imaginary time becomes longer as $t/U_{e\text{-ph}} \to 0$, due to the small tunnel barrier

$$\Delta \tau_{\text{inst}} = \int dX \sqrt{\frac{M}{2\Delta V_{\text{eff}}(X)}} \sim \frac{1}{\hbar\omega_0} \cdot \sqrt{\frac{U_{e\text{-ph}}}{t}}. \quad (17)$$

The fluctuation determinant can be estimated as the ratio between the two harmonic oscillator propagators during the interval $\Delta\tau_{\text{inst}}$ with the dynamical matrix evaluated for an intermediate (initial) X_{middle} (X_{init}) configuration

$$A \sim \left[\frac{\det\left(-\partial_\tau^2 + \frac{1}{M}V_{\text{eff}}''[X_{\text{middle}}]\right)\big|_{(0,\Delta\tau_{\text{inst}})}}{\det\left(-\partial_\tau^2 + \frac{1}{M}V_{\text{eff}}''[X_{\text{init}}]\right)\big|_{(0,\Delta\tau_{\text{inst}})}} \right]^{-\frac{1}{2}}$$

$$= \left(\prod_n \frac{\omega_{\text{middle}}^{(n)}}{\omega_{\text{init}}^{(n)}} \frac{\sinh\left(\hbar\omega_{\text{init}}^{(n)}\Delta\tau_{\text{inst}}\right)}{\sinh\left(\hbar\omega_{\text{middle}}^{(n)}\Delta\tau_{\text{inst}}\right)} \right)^{1/2}$$

$$\sim \left(\frac{t}{U_{e\text{-ph}}} \right)^{3/4} \exp\left[\# \cdot \sqrt{\frac{U_{e\text{-ph}}}{t}} \right]. \quad (18)$$

In the first line, $\det(...)|_{(0,\Delta\tau_{\text{inst}})}$ denotes that the eigenvalues of the differential operator must be obtained with the boundary condition $\delta X(0) = \delta X(\Delta\tau_{\text{inst}}) = 0$, where $\delta X(\tau)$ denotes the fluctuation coordinate $X(\tau) = X_{\text{cl}}(\tau) + \delta X(\tau)$. The second line is the exact form of the harmonic oscillator propagator, where $\omega_{\text{init}}^{(n)}$ and $\omega_{\text{middle}}^{(n)}$ are the square root eigenvalues of the respective dynamical matrices $\frac{1}{M}V_{\text{eff}}''[X_{\text{init}}]$ and $\frac{1}{M}V_{\text{eff}}''[X_{\text{middle}}]$. In the third line, we used the fact that there are three (six) nearly zero oscillator frequencies $\omega_{\text{init}}^{(n)}$ ($\omega_{\text{middle}}^{(n)}$)

of order $O(\sqrt{\frac{t}{U_{e\text{-ph}}}}\omega_0)$, and in general Re $\sum_n(\omega_{\text{init}}^{(n)} - \omega_{\text{middle}}^{(n)}) = O(\omega_0)$. As shown in Fig. 4, the asymptotic behavior extracted from numerical calculation fits well with the asymptotic form Eq. (18).

These asymptotic behaviors lead to an unconventional scaling of T_c of the bipolaronic superconductor

$$T_c \sim t \sqrt{\frac{\hbar\omega_0}{U_{e\text{-ph}}}} \exp\left[-3.2 \frac{\sqrt{t U_{e\text{-ph}}}}{\hbar\omega_0} + 0.46 \sqrt{\frac{U_{e\text{-ph}}}{t}} \right], \quad (19)$$

which is valid when $\hbar\omega_0 \ll t \ll U_{e\text{-ph}}$ (see below for justification) and is parametrically larger, for the same set of parameters, than that obtained in the Holstein model: $T_c^{\text{Holstein}} \sim \frac{t^2}{\sqrt{U_{e\text{-ph}}\hbar\omega_0}} \exp[-\frac{2U_{e\text{-ph}}}{\hbar\omega_0}]$ [45] Note the huge reduction due to the exponent. We consider this a fair comparison as $U_{e\text{-ph}}$ is the binding energy of the bipolaron in both models in the atomic limit.

Validity of the approximations. Our theory is based on two approximations, which can be justified as long as certain parameter conditions are satisfied.

The first is the adiabatic approximation, i.e., the assumption that electronic states adiabatically follow the instantaneous ground state corresponding to the phonon configurations, which is justified as long as [46]

$$\frac{|\langle\Psi^0(\tau)|\partial_\tau \hat{H}_e|\Psi^n(\tau)\rangle|}{\Delta_{0n}^2} \ll 1, \quad (20)$$

where $\hat{H}_e(\tau)$ denotes the instantaneous electronic Hamiltonian, $\Psi^n(\tau)$ is its nth eigenstate, and $\Delta_{0n}(\tau) \equiv E_n(\tau) - E_0(\tau)$ is an instantaneous gap between nth excited state and the ground state (τ here is the imaginary time). To ensure this is satisfied, we note that $\frac{|\langle\Psi^0|\partial_\tau \hat{H}_e|\Psi^n\rangle|}{\Delta_{0n}^2(t)} \lesssim \frac{\alpha|\dot{X}|}{\Delta_{\min}^2}$, where $\Delta_{\min}$ is the minimum energy gap along the trajectory and $|\dot{X}|$ is the speed associated with the coordinates $\{X_{\langle ij\rangle}\}$. The phonon trajectory reaches maximum speed when the coordinates are at the position of the largest energy barrier, and the maximum value of the speed becomes $|\dot{X}|_{\max} = \sqrt{\frac{2\Delta V_{\text{eff}}}{M}}$, where ΔV_{eff} is the height of the energy barrier. Thus, a sufficient condition for the adiabatic theorem to be valid in our treatment is

$$\frac{\hbar\omega_0}{U_{e\text{-ph}}} \ll \frac{\Delta_{\min}^2}{\sqrt{\Delta V_{\text{eff}} U_{e\text{-ph}}^3}}. \quad (21)$$

The second instanton approximation is, technically speaking, a semiclassical approximation of the tunneling event, which is valid when the saddle point contribution dominates the path integral:

$$S_{\text{inst}} \gg |\ln(A)|. \quad (22)$$

For $t/U_{e\text{-ph}} \ll 1$, this amounts to the condition $t \gg \hbar\omega_0$, whereas for $t/U_{e\text{-ph}} = O(1)$, it requires $U_{e\text{-ph}} \gg \hbar\omega_0$ [given that both $\tilde{S} = S_{\text{inst}}\hbar\omega_0/U_{e\text{-ph}}$ and $\ln(A)$ are $O(1)$].

In our numerical simulation of the instanton processes, we find that the adiabaticity condition, Eq. (21), is always

satisfied whenever Eq. (22) is satisfied. Therefore, in the semiclassical limit properly defined in Eq. (22), our results are asymptotically exact.

[1] X. Zhou, W.-S. Lee, M. Imada, N. Trivedi, P. Phillips, H.-Y. Kee, P. Törmä, and M. Eremets, High-temperature superconductivity, Nat. Rev. Phys. **3**, 462 (2021).

[2] B. K. Chakraverty, Possibility of insulator to superconductor phase transition, J. Phys. Lett. **40**, 99 (1979).

[3] B. Chakraverty, D. Feinberg, Z. Hang, and M. Avignon, Squeezed bipolaronic states and high temperature superconductivity in BaLaCuO systems, Solid State Commun. **64**, 1147 (1987).

[4] J. Bonča, T. Katrasňik, and S. A. Trugman, Mobile bipolaron, Phys. Rev. Lett. **84**, 3153 (2000).

[5] A. S. Alexandrov, Breakdown of the Migdal-Eliashberg theory in the strong-coupling adiabatic regime, Europhys. Lett. **56**, 92 (2001).

[6] I. Esterlis, B. Nosarzewski, E. W. Huang, B. Moritz, T. P. Devereaux, D. J. Scalapino, and S. A. Kivelson, Breakdown of the Migdal-Eliashberg theory: A determinant quantum Monte Carlo study, Phys. Rev. B **97**, 140501(R) (2018).

[7] I. Esterlis, S. A. Kivelson, and D. J. Scalapino, Pseudogap crossover in the electron-phonon system, Phys. Rev. B **99**, 174516 (2019).

[8] J. E. Moussa and M. L. Cohen, Two bounds on the maximum phonon-mediated superconducting transition temperature, Phys. Rev. B **74**, 094520 (2006).

[9] I. Esterlis, S. A. Kivelson, and D. J. Scalapino, A bound on the superconducting transition temperature, npj Quantum Mater. **3**, 59 (2018).

[10] J. S. Hofmann, D. Chowdhury, S. A. Kivelson, and E. Berg, Heuristic bounds on superconductivity and how to exceed them, npj Quantum Mater. **7**, 83 (2022).

[11] A. V. Chubukov, A. Abanov, I. Esterlis, and S. A. Kivelson, Eliashberg theory of phonon-mediated superconductivity — When it is valid and how it breaks down, Ann. Phys. **417**, 168190 (2020).

[12] C. Zhang, J. Sous, D. R. Reichman, M. Berciu, A. J. Millis, N. V. Prokof'ev, and B. V. Svistunov, Bipolaronic high-temperature superconductivity, Phys. Rev. X **13**, 011010 (2023).

[13] J. Sous, C. Zhang, M. Berciu, D. R. Reichman, B. V. Svistunov, N. V. Prokof'ev, and A. J. Millis, Bipolaronic superconductivity out of a Coulomb gas, Phys. Rev. B **108**, L220502 (2023).

[14] J. Sous, M. Chakraborty, R. V. Krems, and M. Berciu, Light bipolarons stabilized by Peierls electron-phonon coupling, Phys. Rev. Lett. **121**, 247001 (2018).

[15] H.-X. Wang, Y.-F. Jiang, and H. Yao, Robust d-wave superconductivity from the Su-Schrieffer-Heeger-Hubbard model: possible route to high-temperature superconductivity, arXiv:2211.09143.

[16] A. Tanjaroon Ly, B. Cohen-Stead, S. Malkaruge Costa, and S. Johnston, Comparative study of the superconductivity in the holstein and optical Su-Schrieffer-Heeger models, Phys. Rev. B **108**, 184501 (2023).

[17] X. Cai, Z.-X. Li, and H. Yao, High-temperature superconductivity induced by the Su-Schrieffer-Heeger electron-phonon coupling, arXiv:2308.06222.

[18] J. Sous and M. Pretko, Fractons from polarons, Phys. Rev. B **102**, 214437 (2020).

[19] M. R. Carbone, A. J. Millis, D. R. Reichman, and J. Sous, Bond-Peierls polaron: Moderate mass enhancement and current-carrying ground state, Phys. Rev. B **104**, L140307 (2021).

[20] B. Xing, W.-T. Chiu, D. Poletti, R. T. Scalettar, and G. Batrouni, Quantum Monte Carlo simulations of the 2D Su-Schrieffer-Heeger model, Phys. Rev. Lett. **126**, 017601 (2021).

[21] X. Cai, Z.-X. Li, and H. Yao, Antiferromagnetism Induced by Bond Su-Schrieffer-Heeger Electron-Phonon Coupling: A Quantum Monte Carlo Study, Phys. Rev. Lett. **127**, 247203 (2021).

[22] C. Feng, B. Xing, D. Poletti, R. Scalettar, and G. Batrouni, Phase diagram of the Su-Schrieffer-Heeger-hubbard model on a square lattice, Phys. Rev. B **106**, L081114 (2022).

[23] X. Cai, Z.-X. Li, and H. Yao, Robustness of antiferromagnetism in the Su-Schrieffer-Heeger Hubbard model, Phys. Rev. B **106**, L081115 (2022).

[24] A. Götz, S. Beyl, M. Hohenadler, and F. F. Assaad, Valence-bond solid to antiferromagnet transition in the two-dimensional Su-Schrieffer-Heeger model by Langevin dynamics, Phys. Rev. B **105**, 085151 (2022).

[25] Z. Han and S. A. Kivelson, Resonating valence bond states in an electron-phonon system, Phys. Rev. Lett. **130**, 186404 (2023).

[26] A. Götz, M. Hohenadler, and F. F. Assaad, Phases and exotic phase transitions of a two-dimensional Su-Schrieffer-Heeger model, Phys. Rev. B **109**, 195154 (2024).

[27] S. Malkaruge Costa, B. Cohen-Stead, A. T. Ly, J. Neuhaus, and S. Johnston, Comparative determinant quantum Monte Carlo study of the acoustic and optical variants of the Su-Schrieffer-Heeger model, Phys. Rev. B **108**, 165138 (2023).

[28] B. Xing, C. Feng, R. Scalettar, G. G. Batrouni, and D. Poletti, Attractive Su-Schrieffer-Heeger-Hubbard model on a square lattice away from half-filling, Phys. Rev. B **108**, L161103 (2023).

[29] Q.-G. Yang, M. Yao, D. Wang, and Q.-H. Wang, Charge bond order and s-wave superconductivity in the kagome lattice with electron-phonon coupling and electron-electron interaction, Phys. Rev. B **109**, 075130 (2024).

[30] X. Cai, Z. Han, Z.-X. Li, S. A. Kivelson, and H. Yao, Quantum spin liquid from strong electron-phonon coupling (unpublished).

[31] Z. Han and S. Kivelson, Emergent gauge fields in band insulators, arXiv:2405.17539.

[32] This can be most easily seen by rescaling the phonon coordinates $\hat{X} \to \frac{\alpha}{K}\hat{X}$ in the Hamiltonian, rendering them dimensionless.

[33] D. S. Fisher and P. C. Hohenberg, Dilute Bose gas in two dimensions, Phys. Rev. B **37**, 4936 (1988).

[34] N. Prokof'ev, O. Ruebenacker, and B. Svistunov, Critical point of a weakly interacting two-dimensional Bose gas, Phys. Rev. Lett. **87**, 270402 (2001).

[35] S. Pilati, S. Giorgini, and N. Prokof'ev, Critical temperature of interacting Bose gases in two and three dimensions, Phys. Rev. Lett. **100**, 140405 (2008).

[36] P. K. Mogensen and A. N. Riseth, Optim: A mathematical optimization package for Julia, J. Open Source Softw. **3**, 615 (2018).

[37] N. C. Murphy, R. Wortis, and W. A. Atkinson, Generalized inverse participation ratio as a possible measure of localization for interacting systems, Phys. Rev. B **83**, 184206 (2011).

[38] Due to limitations of numerical resources, we only calculate the properties of bipolarons for the range $0 < t/U_{e\text{-ph}} \leqslant 0.7$ As $t/U_{e\text{-ph}}$ grows, our numerics do not converge well for systems larger than 70×70. We also note that it is likely that static bipolarons become fully delocalized throughout the entire system at some critical value of $t/U_{e\text{-ph}}$ beyond which our method breaks down.

[39] A. Nocera, J. Sous, A. E. Feiguin, and M. Berciu, Bipolaron liquids at strong Peierls electron-phonon couplings, Phys. Rev. B **104**, L201109 (2021).

[40] A. Altland and B. D. Simons, *Condensed Matter Field Theory*, 2nd ed. (Cambridge University Press, Cambridge, UK, 2010).

[41] S. Coleman, *Aspects of Symmetry: Selected Erice Lectures* (Cambridge University Press, Cambridge, UK, 1988).

[42] J. Zinn-Justin, *Quantum Field Theory and Critical Phenomena* (Oxford University Press, Oxford, UK, 2021).

[43] K. Voelker and S. Chakravarty, Multiparticle ring exchange in the Wigner glass and its possible relevance to strongly interacting two-dimensional electron systems in the presence of disorder, Phys. Rev. B **64**, 235125 (2001).

[44] K.-S. Kim, I. Esterlis, C. Murthy, and S. A. Kivelson, Dynamical defects in a two-dimensional Wigner crystal: self-doping and kinetic magnetism, Phys. Rev. Lett. **132**, 133402 (2024).

[45] Z. Han, S. A. Kivelson, and H. Yao, Strong coupling limit of the Holstein-Hubbard model, Phys. Rev. Lett. **125**, 167001 (2020).

[46] M. H. S. Amin, Consistency of the adiabatic theorem, Phys. Rev. Lett. **102**, 220401 (2009).